Communication: Probing the existence of partially arrested states in ionic liquids

Pedro E. Ramírez-González, Luis E. Sanchéz-Díaz, Magdaleno Medina-Noyola, and Yanting Wang

Articles you may be interested in

Rigidity and soft percolation in the glass transition of an atomistic model of ionic liquid, 1-ethyl-3-methyl imidazolium nitrate, from molecular dynamics simulations—Existence of infinite overlapping networks in a fragile ionic liquid
J. Chem. Phys. **142**, 164501 (2015); 10.1063/1.4918586

Manifestations of probe presence on probe dynamics in supercooled liquids
J. Chem. Phys. **135**, 214503 (2011); 10.1063/1.3664125

Ab initio molecular dynamics simulation of ionic liquids
J. Chem. Phys. **126**, 154502 (2007); 10.1063/1.2718531

Collective excitations in an ionic liquid
J. Chem. Phys. **124**, 074513 (2006); 10.1063/1.2172602

Dynamic arrest in a liquid of symmetric dumbbells: Reorientational hopping for small molecular elongations
J. Chem. Phys. **123**, 204505 (2005); 10.1063/1.2085030

Communication: Probing the existence of partially arrested states in ionic liquids

Pedro E. Ramírez-González,[1] Luis E. Sanchéz-Díaz,[2] Magdaleno Medina-Noyola,[3] and Yanting Wang[4,5]

[1]*CONACYT - Instituto de Física "Manuel Sandoval Vallarta," Universidad Autónoma de San Luis Potosí, Álvaro Obregón 64, 78000 San Luis Potosí, SLP, Mexico*
[2]*Department of Materials Science and Engineering, University of Tennessee, Knoxville, Tennessee 37996, USA*
[3]*Instituto de Física "Manuel Sandoval Vallarta," Universidad Autónoma de San Luis Potosí, Álvaro Obregón 64, 78000 San Luis Potosí, SLP, Mexico*
[4]*State Key Laboratory of Theoretical Physics, Institute of Theoretical Physics, Chinese Academy of Sciences, 55 East Zhongguancun Road, P.O. Box 2735, Beijing 100190, China*
[5]*School of Physical Sciences, University of Chinese Academy of Sciences, 19A Yuquan Road, Beijing 100049, China*

The recent predictions of the self-consistent generalized Langevin equation theory, describing the existence of unusual partially arrested states in the context of ionic liquids, were probed using all-atom molecular dynamics simulations of a room-temperature ionic liquid. We have found a slower diffusion of the smaller anions compared with the large cations for a wide range of temperatures. The arrest mechanism consists on the formation of a strongly repulsive glass by the anions, stabilized by the long range electrostatic potential. The diffusion of the less repulsive cations occurs through the holes left by the small particles. All of our observations in the simulated system coincide with the theoretical picture. *Published by AIP Publishing.* [http://dx.doi.org/10.1063/1.4967518]

Understanding all aspects of glass transition is one of the great challenges in modern science.[1–3] Despite much research having been done in recent years,[4] the possibility of observing mixed arrested states, in which only one of the components becomes glass while the rest of the system remains fluid, has received less attention.[5]

Recently, the Self-Consistent Generalized Langevin Equation (SCGLE) theory was used to investigate the dynamically arrested states in the context of the primitive model (PM) of molten salts.[6] The most important result of the cited work was the prediction of low-temperature regions where the larger ions are fluid and the smaller ions are arrested. These domains of mixed states are related with the size and charge asymmetries between ions and are accessible at very low temperatures.

Such kind of partially arrested states has been observed in materials known as superionic conductors,[7] in which one type of the constitutive ions is able to move inside the solid matrix formed by the other components. Crystalline and glassy superionic conductors were extensively used in the industry of batteries since the 1980s.[8] However, superionic conductors used to have a very complex composition, making difficult their direct comparison with our theoretical approach. Curiously, a novel class of ionic fluids, known as Room-Temperature Ionic Liquids (RTIL), possesses a glassy-behavior at room temperatures and resulted more adequate for probing the theoretical predictions.[9,10] Clearly, due to that both systems are Coulombic fluids, most of the conclusions obtained in RTIL can be applied to superionic conductors.

RTIL are compounds usually formed by large organic cations combined with organic or inorganic anions which melt at temperatures less than $100\,^\circ$C.[11] The study of these solvents has become very active due to their potential applicability towards industry.[12] Despite the intense research around RTIL, scarce investigation has been done with respect to their glassy behavior.[10,13–21] Many researchers have previously observed a slower diffusion of the smaller anions in RTIL, either by experiments[21] or by molecular dynamics (MD) simulations.[10,13–20] The most common explanation appeals to the dynamics along the direction of the carbon located between the two nitrogens in the imidazolium ring with a marginal dependence on the anion.[22,23] However, the present work offers an alternative explanation for this observation on RTIL, one that is supported by an analysis of the simulation results in light of the SCGLE theoretical predictions. The existence of partially arrested states in RTIL may open the possibility for developing novel conducting materials near room temperature.

We studied the glassy behavior of the *generic* RTIL 1-ethyl-3-methyl-imidazolium tetrafluoroborate (EMIM$^+$-BF$_4^-$) using all-atom molecular dynamics (MD) simulations. For this particular compound, we have observed the onset in the formation of partially arrested states in which the small anion (BF$_4^-$) becomes arrested while the large cation (EMIM$^+$) is still fluid. In addition, a qualitative comparison between theory and simulation is presented in order to contrast with the general picture given by theoretical predictions. We can conclude that the partially arrested states in ionic liquids previously predicted by the SCGLE theory are consistent with our MD simulations of EMIM$^+$-BF$_4^-$.

The SCGLE theory of dynamic arrest leads to a remarkably simple equation for the asymptotic value $\gamma_\alpha \equiv \lim_{t\to\infty} \langle (\Delta R^{(\alpha)})^2 \rangle$ of the mean-squared displacement

145, 191101-1

(MSD) of particles of species α. This property constitutes a convenient parameter with which to describe dynamic arrest in mixtures, since it indicates if the particles of certain species diffuse (infinite value of γ_α) or are arrested (finite value of γ_α). The existence of a partially arrested state implies the arrest of one component and the diffusion of the other one. The referred equation reads as[24]

$$\frac{1}{\gamma_\alpha} = \frac{1}{3(2\pi)^3} \int d^3k k^2 \left\{ \lambda[\lambda + k^2\gamma]^{-1} \right\}_{\alpha\alpha}$$
$$\times \left\{ c\sqrt{n}S\lambda[S\lambda + k^2\gamma]^{-1}\sqrt{n}h \right\}_{\alpha\alpha}, \quad (1)$$

where S is the matrix of partial structure factors and h and c are the Ornstein-Zernike (OZ) matrices of total and direct correlation functions, respectively. The matrix $\sqrt{n}$ is defined as $[\sqrt{n}]_{\alpha\beta} \equiv \delta_{\alpha\beta}\sqrt{n_\alpha}$, and $\lambda(k)$ is a diagonal matrix given by $\lambda_{\alpha\beta}(k) = \delta_{\alpha\beta}\left[1 + (k/k_c^{(\alpha)})^2\right]^{-1}$, with $k_c^{(\alpha)} = 8.17/\sigma_\alpha$.

We used a model of charged hard spheres, usually referred to as the primitive model (PM), for which the analytical solution of the OZ equation was given by Blum under the mean-sphere approximation (MSA).[25]

We have performed all-atom MD simulations of ionic liquid EMIM$^+$-BF$_4^-$ using the MD package GROMACS.[26] The BF$_4^-$ anion has a tetrahedron structure and a mean size of 0.19 nm, while the EMIM$^+$ cation is essentially planar and with a maximum size (taken from methyl to ethyl) of ~0.69 nm (see Fig. 1). The force field of EMIM$^+$ is based on the AMBER potential,[27] and the BF$_4^-$ force field was developed by de Andrade and colleagues.[28] Periodic boundary conditions were applied to the three dimensions with a 1.6 nm cutoff for the atomic interactions. The long-range electrostatic interactions were handled with the particle mesh Ewald method.[29] As an initial configuration for the EMIM$^+$-BF$_4^-$ RTIL, we have used a simulation box with 1024 ion pairs randomly positioned.

The equilibration procedure is the same as described in Ref. 30. The equilibrated sample was probed from 700 K to 250 K in temperature steps of $\Delta T = 50$ K. We simulated the system for a duration of 10 ns (10 000 configurations) at each temperature for the calculation of the mean-square displacement (MSD), the diffusion coefficient, and the radial distribution functions (RDFs). For obtaining reliable results at lower temperatures, we have used 100 ns durations for temperatures below 350 K.

Isobaric trajectories ($P = 1$ atm) were used in both simulation and theory. We employed the dimensionless quantities commonly used in the PM for: pressure $P^* \equiv P\epsilon_0\sigma_{bs}^4/e^2$ ($\sigma_{bs} \equiv (\sigma_{big} + \sigma_{small})/2$, where σ_α is the diameter of the corresponding ion), temperature $T^* \equiv k_BT\sigma_{bs}\epsilon_0/e^2$, and total
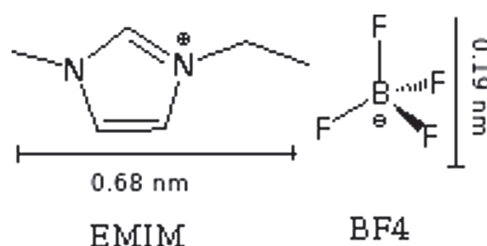
volume fraction $\phi \equiv \pi(n_{big}\sigma_{big}^3 + n_{small}\sigma_{small}^3)/6$. For all the previous definitions, ϵ_0 is the vacuum permittivity, k_B is the Boltzmann constant, e is the electron charge, and n_α corresponds to the number density of particles α. We have chosen a size asymmetry of $\delta = 3.5$ ($\delta = \sigma_{big}/\sigma_{small}$) in our theoretical calculations because it is close to the size ratio between EMIM$^+$ and BF$_4^-$ molecules. Clearly, the simulated ions are not charged hard spheres; therefore, we expect incorrect values of temperature and volume fraction for their dynamic arrest using the PM. However, let us suppose that the essential features of ionic liquids can be described by the PM.

In Fig. 2 we show the dynamic arrest line, calculated with Eq. (1), in terms of variables T^* and ϕ. The solid line corresponds to the transition to fully arrested states (G-G) in which both ions are arrested. The dashed line separates the fluid region from the partially arrested states (F-G) where only one of the components is arrested. The dotted line represents the isobaric trajectory used for our additional theoretical calculations. For reference, we have marked three representative points with large circles corresponding to $T^* = 0.079$, 0.025, and 0.012. In the inset, we plot the inverse of the localization length $1/\gamma_\alpha$ as a function of T^* over the isobaric trajectory. The squares and the circles correspond to the data of the cations (large particles) and anions (small particles), respectively. We can observe that $1/\gamma_{anion}$ becomes different from zero at higher temperatures ($T^* \approx 0.013$) than compared with $1/\gamma_{cation}$ ($T^* \approx 0.01$), indicating that inside the F-G region the anion is arrested and the cations are liquid.

The prediction of partially arrested states is confirmed by observing the inset of Fig. 3, where the mean square displacement (MSD) of the large cations (dashed lines) and small anions (solid lines) at temperatures $T^* = 0.079$, 0.025, and 0.012 are shown. We can observe that, even at temperatures above the dynamic arrest transition ($T^* = 0.079$), the slope of the MSD of the anion has a lower value compared with the slope of the cation. At lower temperatures ($T^* = 0.025$), the difference between the slopes increases. Finally, inside region
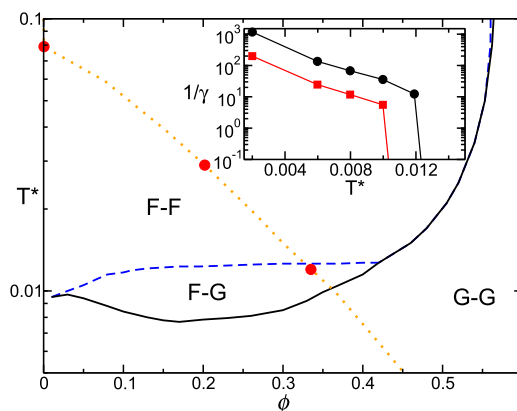

FIG. 2. Arrest lines predicted by the SCGLE theory for the PM with a size asymmetry adequate for the simulated RTIL (1:3.5). The fluid region is labeled as F-F. The G-G region corresponds to fully arrested states. Inside the F-G region we found partially arrested. The dotted line is an isobaric trajectory equivalent to 1 atm of pressure. The points over the dotted line correspond to the following effective temperatures $T^* = 0.079$, 0.025, and 0.012. In the inset we plot the values of the parameter $1/\gamma_\alpha$ following the isobaric trajectory. Circles correspond to anions (small particles) and squares to cations (large particles).
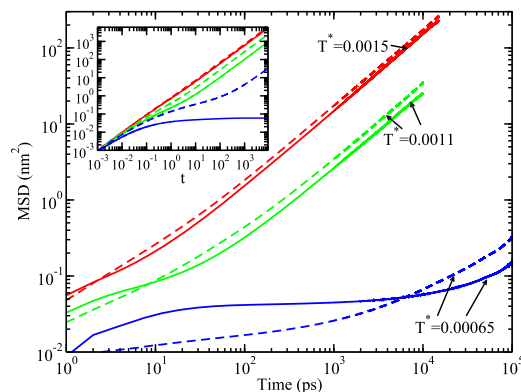

FIG. 1. Schematic representation of the ions studied by MD simulation.

FIG. 3. MSD of EMIM$^+$-BF$_4^-$ for the temperatures $T^* = 0.0015$ (700 K), 0.0011 (500 K), and 0.00065 (300 K). Dashed lines represent our results for the cations and solid lines represent anions. At the lower temperature, the anion in MSD is almost bounded, indicating dynamic arrest. Inset: Theoretical calculations of the mean-square displacement for $T^* = 0.079, 0.025$, and 0.012 over the isobaric trajectory used in this work (big circles in Fig. 2). The first two temperatures are located in the F-F region and the last one inside the F-G region. Solid and dashed lines correspond to anions and cations, respectively.

FIG. 4. Diffusion coefficient as a function of the temperature of the EMIM$^+$-BF$_4^-$ system. Lower diffusion coefficients were observed for the BF$_4^-$ anion in a wide range of temperatures. Empty symbols represent experimental measurements showing the same tendency.[21] Inset: Theoretical calculation of the diffusion coefficient as a function of T^* in the context of the primitive model. The solid line corresponds to the diffusion coefficient of anions and the dashed line to cations.

F-G ($T^* = 0.012$) the anions become arrested while the cations remain mobile.

The main panel of Fig. 3 contains our MD simulation results for the MSD. We show our calculations for three representative temperatures, i.e., $T^* = 0.0015$ (700 K), 0.0011 (500 K), and 0.00065 (300 K). The solid and dashed lines correspond to the MSD of the BF$_4^-$ anion (small particles) and the EMIM$^+$ cation (large particles), respectively. At short times, we observe a faster mobility of BF$_4^-$ compared with EMIM$^+$ due to that, in the ballistic regime, the molecules perform a free flight dominated by the thermal velocity $v_T = \sqrt{K_B T/M}$, which is scaled with the mass of the molecules. Hence, the massive EMIM$^+$ (~111 amu) moves slower than BF$_4^-$ (~87 amu). However, in the diffusive regime (long time) the molecular collisions dominate, and the diffusion of BF$_4^-$ becomes slower than the EMIM$^+$ diffusion. The differences between theory and simulations for short times are due to lacking of the ballistic regime in the SCGLE theory (originally developed for describing colloids). However, the dynamic arrest transition is a long-time effect. Thus, the behavior of the simulated RTIL at large times essentially reproduces the theoretical predictions for the PM.

The full squares in Fig. 4 correspond to our MD results of the diffusion coefficient of anions and the full circles to the cations, the lines are only guides for the eye. The intuitive idea that bigger particles have slower diffusion contrasts with the observed faster diffusion of the bigger EMIM$^+$ in our MD simulations. In order to reinforce the validity of our results, we included experimental measurements (empty symbols) of diffusion coefficients (taken from Ref. 21), which confirms the tendency observed in the simulations. The comparison between simulation and experiments may be improved upon using polarizable force fields, for which the net effect is that the system becomes more mobile.[31–33] However, the complexity of the force fields is surely not affecting the observation of anomalous diffusion of RTIL.

As reference, the inset of Fig. 4 shows the SCGLE calculation of the self-diffusion coefficient as a function of T^* over the isobaric trajectory, which crosses through the F-C region. The
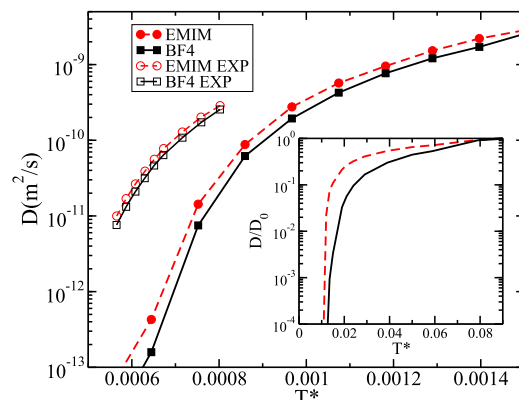
solid line corresponds to the diffusion coefficient of cations and the dashed line to that of anions. We can observe that the diffusion coefficient vanishes at higher temperature for the anions than for the cations, implying the arrest of the anions and the diffusion of the larger cations. Despite the complexity of the constituent ions of RTIL and the fact that we have performed all-atom simulations, both simulations and experiments are in complete qualitative agreement with the predictions of the SCGLE theory. The evidence presented above shows the existence of partially arrested states in RTIL, where the small particles are arrested and the large particles are mobile.

In Fig. 5 we show the radial distribution functions (RDFs) for $T^* = 0.0015$ (red), 0.0011 (green), and 0.00065 (blue), where the dashed, dashed-dotted, and solid lines correspond to $g_{+-}(r)$, $g_{++}(r)$, and $g_{--}(r)$, respectively. Notice that the first peak of $g_{+-}(r)$ is located approximately at $r \approx 0.435$ nm and the first peak of $g_{++}(r)$ can be found around 0.7 nm for all the temperatures probed. On the other hand, the first peak position of $g_{--}(r)$ decreases from 0.73 nm to 0.63 nm as temperature lowers. From Fig. 5, we can see that while the $g_{+-}(r)$ peak is located at $r \approx 0.45$ nm $\approx (\sigma_{cation} + \sigma_{anion})/2$ and $g_{++}(r)$ at

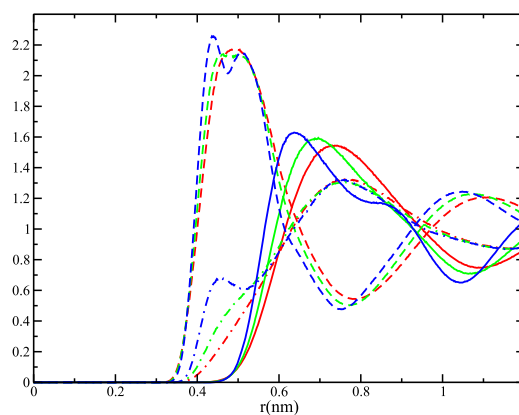FIG. 5. Radial distribution functions for EMIM$^+$-BF$_4^-$. The dashed, dashed-dotted, and solid lines represent $g_{+-}(r)$, $g_{++}(r)$, and $g_{--}(r)$, respectively. We have plotted three representative temperatures, i.e., $T^* = 0.0015$ (red), 0.0011 (green), and 0.00065 (blue).
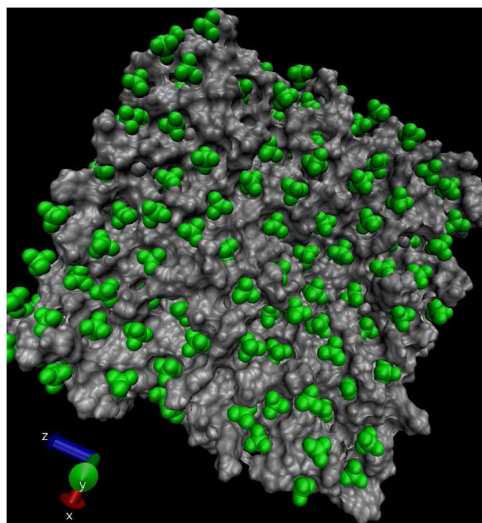
FIG. 6. Snapshot of the system at $T^* = 0.000\,65$. The green particles are the anions and the continuous gray surface represents the space occupied by the cations.

$r \approx 0.68$ nm $\approx \sigma_{cation}$, the first peak of $g_{--}(r)$ is located in between 0.6 nm and 0.7 nm which is larger than σ_{anion}. This behavior is typical of a Wigner glass in which the mean distance of the constituents of the glass is very large.[34]

What we are observing is that the cations have a low efficiency on screening the charge of the anions, due to their large volume, which implies that the anion-anion repulsion is greater than the cation-cation repulsion. In consequence, the anions become a glass due to the high repulsion between them, and the less repulsive cations have enough space for diffusion.

In Fig. 6 we show a snapshot of the system at $T^* = 0.000\,65$. The BF_4^- anions are colored with green and the cations are represented as a continuous gray surface. We can observe that the mean distance of the anions is very large, showing the formation of a strongly repulsive glass. The space between the anions makes possible the diffusion of the less repulsive cations.

In the present work we have probed the predictions of the SCGLE about the existence of partially arrested states at low temperatures in the context of ionic liquids using all-atom molecular dynamic simulations of $EMIM^+$-BF_4^- ionic liquid. The predicted arrested states are characterized by an atypical behavior in which the small particles, the anions in this case, are arrested while the large particles remain mobile. We have found that the essential features predicted by the SCGLE theory in the onset of glass transition were observed in our simulated RTIL. The most important common features are the following: (1) the diffusion of the anions, observed in the MSD and the diffusion coefficient, is slower for a wide range of temperatures and (2) the MSD of the anions becomes almost bounded at a higher temperature than the cations. In addition, we can propose the formation of a strongly repulsive glass by the anions as the arrest mechanism in these unusual states.

The qualitative agreement between the theoretical prediction of these singular arrested states with simulation and experimental results gives a proof of the reliability of the theoretical predictions.

[1] F. H. Stillinger and P. G. Debenedetti, Annu. Rev. Condens. Matter Phys. **4**, 263 (2013).
[2] P. G. Debenedetti and F. H. Stillinger, Nature **410**, 259 (2001).
[3] C. A. Angell, K. L. Ngai, G. B. McKenna, P. F. McMillan, and S. W. Martin, J. Appl. Phys. **88**, 3113 (2000).
[4] L. Berthier and G. Biroli, Rev. Mod. Phys. **83**, 587 (2011).
[5] J. Hendricks, R. Capellmann, A. B. Schofield, S. U. Egelhaaf, and M. Laurati, Phys. Rev. E **91**, 032308 (2015), and references therein.
[6] L. E. Sanchez-Díaz, A. Vizcarra-Rendón, and R. Juárez-Maldonado, Phys. Rev. Lett. **103**, 035701 (2009).
[7] A. Laskar, *Superionic Solids and Solid Electrolytes Recent Trends* (Elsevier, 2012).
[8] A. Varzi, R. Raccichini, S. Passerini, and B. Scrosati, "Challenges and prospects of the role of solid electrolytes in the revitalization of lithium metal batteries," J. Mater. Chem. A (published online).
[9] M. G. Del Popolo and G. A. Voth, J. Phys. Chem. B **108**, 1744 (2004).
[10] J. Habasaki and K. L. Ngai, J. Chem. Phys. **142**, 164501 (2015).
[11] W. Freyland, *Coulombic Fluids: Bluk and Interfaces* (Springer, 2011).
[12] N. V. Plechkova and K. R. Seddon, Chem. Soc. Rev. **37**, 123 (2008).
[13] A. Triolo *et al.*, J. Phys. Chem. B **110**, 21357 (2006); K. R. Harris, L. A. Woolf, and M. Kanakubo, J. Chem. Eng. Data **50**, 1777 (2005).
[14] J. Habasaki and K. L. Ngai, Anal. Sci. **24**, 1321 (2008).
[15] J. Habasaki and K. L. Ngai, J. Chem. Phys. **129**, 194501 (2008).
[16] J. Habasaki and K. L. Ngai, J. Non-Cryst. Sol. **357**, 446 (2011).
[17] N. C. Forero-Martinez, R. Cortes-Huerto, and P. Ballone, J. Chem. Phys. **136**, 204510 (2012).
[18] O. Andreussi and N. Marzari, J. Chem. Phys. **137**, 044508 (2012).
[19] M. H. Kowsari, S. Alavi, M. Ashrafizaadeh, and B. Najafi, J. Chem. Phys. **129**, 224508 (2008).
[20] H. A. Every, A. G. Bishop, D. R. MacFarlane, G. Oradd, and M. Forsyth, Phys. Chem. Chem. Phys. **6**, 1758 (2004).
[21] A. Noda, K. Hayamizu, and M. Watanabe, J. Phys. Chem. B **105**, 4603 (2001).
[22] S. M. Urahata and M. C. C. Ribeiro, J. Chem. Phys. **120**, 1855 (2004).
[23] S. M. Urahata and M. C. C. Ribeiro, J. Chem. Phys. **122**, 024511 (2005).
[24] R. Juarez-Maldonado and M. Medina-Noyola, Phys. Rev. E **77**, 051503 (2008).
[25] L. Blum, Mol. Phys. **30**, 1529 (1975).
[26] H. J. C. Berendsen, D. Vanderspoel, and R. Vandrunen, Comput. Phys. Commun. **91**, 43 (1995).
[27] W. D. Cornell *et al.*, J. Am. Chem. Soc. **117**, 5179 (1995).
[28] J. de Andrade, E. S. Boes, and H. Stassen, J. Phys. Chem. B **106**, 13344 (2002).
[29] U. Essmann, L. Perera, M. L. Berkowitz, T. Darden, H. Lee, and L. G. Pedersen, J. Chem. Phys. **103**, 8577 (1995).
[30] P. E. Ramírez-González, G. Ren, G. Saielli, and Y. Wang, J. Phys. Chem. B **120**, 5678 (2016).
[31] O. Borodin, J. Phys. Chem. B **113**, 11463 (2009).
[32] T. Yan, Y. Wang, and C. Knox, J. Phys, Chem. B **114**, 6886 (2010).
[33] T. Yan, Y. Wang, and C. Knox, J. Phys. Chem. B **114**, 6905 (2010).
[34] H. Tanaka, J. Meunier, and D. Bonn, Phys. Rev. E **69**, 031404 (2004).